Nasal-associated lymphoid tissue and olfactory epithelium as portals of entry for Burkholderia pseudomallei in murine melioidosis

Author

Owen, Suzzanne, Batzloff, Michael, Chehrehasa, Fatemeh, Meedeniya, Adrian, Casart Quintero, Yveth, Logue, Carie-Anne, Hirst, Robert, Peak, Ian, Mackay-Sim, Alan, Beacham, Ifor

Published

2009

Journal Title

Journal of Infectious Diseases

DOI

10.1086/599210

Nasal-Associated Lymphoid Tissue and Olfactory Epithelium as Portals of Entry for *Burkholderia pseudomallei* in Murine Melioidosis

Suzzanne J. Owen,[1,a] Michael Batzloff,[3,a] Fatemeh Chehrehasa,[2,a] Adrian Meedeniya,[2] Yveth Casart,[1,b] Carie-Anne Logue,[1] Robert G. Hirst,[1] Ian R. Peak,[1] Alan Mackay-Sim,[2] and Ifor R. Beacham[1]

[1]Institute for Glycomics, Griffith University, Gold Coast, [2]Eskitis Institute for Cell and Molecular Therapies, Griffith University, Nathan, and [3]Queensland Institute of Medical Research, Herston, Brisbane, Queensland, Australia.

(See the editorial commentary by Wiersinga and van der Poll, on pages 1720–2.)

Background. *Burkholderia pseudomallei*, the causative agent of melioidosis, is generally considered to be acquired via inhalation of dust or water droplets from the environment. In this study, we show that infection of the nasal mucosa is potentially an important portal of entry in melioidosis.

Methods. After intranasal inoculation of mice, infection was monitored by bioluminescence imaging and by immunohistological analysis of coronal sections. The bacterial loads in organ and tissue specimens were also monitored.

Results. Bioluminescence imaging showed colonization and replication in the nasal cavity, including the nasal-associated lymphoid tissue (NALT). Analysis of coronal sections and immunofluorescence microscopy further demonstrated the presence of infection in the respiratory epithelium and the olfactory epithelium (including associated nerve bundles), as well as in the NALT. Of significance, the olfactory epithelium and the brain were rapidly infected before bacteria were detected in blood, and a capsule-deficient mutant infected the brain without significantly infecting blood.

Conclusions. These data suggest that the olfactory nerve is the route of entry into the brain and that this route of entry may be paralleled in cases of human neurologic melioidosis. This study focuses attention on the upper respiratory tract as a portal of entry, specifically focusing on NALT as a route for the development of systemic infection via the bloodstream and on the olfactory epithelium as a direct route to the brain.

Burkholderia pseudomallei, a member of the β-proteobacteria, is an environmental organism and the causative agent of melioidosis. Melioidosis in humans is a potentially fatal disease with many presentations varying from subacute to chronic and acute disease. Death may occur rapidly after septic shock [1]. The main foci of endemicity are Southeast Asia and northern Australia, where the mortality rates are ~50% and ~20%, respectively [1, 2]. However, melioidosis is also endemic—or is possibly endemic—in many other countries, and is considered to be an emerging disease worldwide [1, 3]. Infections are associated with heavy rainfall and are considered to occur via percutaneous inoculation and by inhalation resulting from aerosolization of the organism [2, 4]. Partly because of the latter route of infection, the lack of a vaccine, a relative resistance to antibiotics, and a capacity for latent infection, *B. pseudomallei* is considered to be a potential bioweapon [3].

A significant characteristic of melioidosis is that virtually any organ may be infected, although the liver, spleen, and lung are most commonly involved [1, 2]. However, neurologic abnormalities and direct invasion of the central nervous system (CNS; i.e., brain stem, cerebellum, and spinal cord) occur in 4% of all cases [5–7]; clinically, ~66% of such cases in Australia may feature brain stem involvement. It has been suggested that *B. pseudomallei* travels along nerves to invade the CNS di-

Received 17 November 2008; accepted 8 January 2009; electronically published 21 May 2009.

Potential conflicts of interest: none reported.

Financial support: National Health and Medical Research Council (grant 326208); Griffith Medical Research College; Australian Department of Health and Ageing (grant to A.M.-S.).

[a] S.J.O., M.B., and F.C. contributed equally to this work.

[b] Present affiliation: Departamento de Biología Estructural, Instituto Venezolano de Investigaciones Científicas, Caracas, Venezuela.

Reprints or correspondence: Prof. Ifor R. Beacham, Institute for Glycomics, Griffith University, Gold Coast, Queensland, Australia (i.beacham@griffith.edu.au).

The Journal of Infectious Diseases 2009; 199:1761–70

0022-1899/2009/19912-0008$15.00
DOI: 10.1086/599210

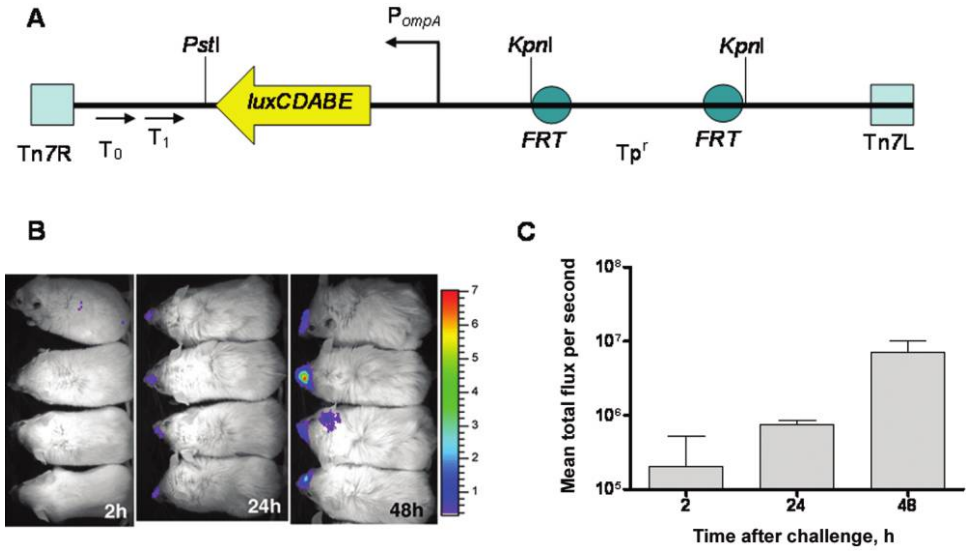

Figure 1. Bioluminescence imaging of mice. *A,* Tn7 transposon that contained the *lux* operon. T_1 and T_0 are T7 terminators. The promoter region from *ompA* (pOmpA) is located upstream of the *lux* operon. *B,* Bioluminescence imaging of mice after intranasal inoculation (by 2 h after inoculation) and at 24-h intervals thereafter. *C,* Quantification of light emission from the nasal region of 4 mice, as determined using LivingImage software (Xenogen). Data are shown as the mean number of photons per second ± the standard deviation.

rectly, whereas brain abscesses may occur via hematogenous spread [5].

Murine melioidosis is widely used to study infection due to *B. pseudomallei.* The BALB/c mouse is considered to model the acute form of the disease, whereas the C57BL/6 mouse is considered to model a chronic form of the disease [8, 9]. In the present study, we investigated infection of BALB/c mice by *B. pseudomallei* with the use of a stable chromosomally integrated *lux*-positive operon, which allowed observation of infection in live animals and detection of sites of infection in situ after dissection [10–12]. After intranasal inoculation of Lux-positive *B. pseudomallei,* rapid replication occurred in the nasal mucosa. Additional studies of coronal sections that were performed using immunofluorescence microscopy demonstrated rapid major infection and invasion of the olfactory epithelium and the nasal-associated lymphoid tissue (NALT) and, surprisingly, rapid colonization of the olfactory brain.

MATERIALS AND METHODS

Bacterial strains and growth conditions. *B. pseudomallei* strains 08, K96243, and 1026b are clinical isolates from Australia (strain 08) and Thailand [13–15]. An allele replacement capsule-deficient mutant of 08 (08Δ*cap*) was generated as described elsewhere [16], by deletion of an 8565-bp region that contained and included *wcbD* to *wcbI* (corresponding to nucleotides 3345928–3354492 of chromosome 1) and was replaced with a tetracycline cassette. *B. pseudomallei* and *Escherichia coli* strains were grown in liquid Luria broth (LB) media with shaking or on LB agar plates. Streptomycin and trimethoprim (Tp; 100 μg/mL) were added when appropriate.

Derivation and in vitro stability of* B. pseudomallei *that expresses the* lux *operon. The promoter region from the *B. pseudomallei ompA* gene (BPSL2522) was amplified as a 188-bp *Kpn*I-*Xho*I fragment by use of the following upstream and downstream primers, respectively, with the requisite restriction sites (underlined) incorporated: GGGGTACCAGACCGATGTTAGGGTGGGG and CCGCTCGAGTGAGATTACCGCAGGTTTACTG. This fragment was then cloned in front of the *luxCDABE* operon from *Photorhabdus luminscens* Hb [17] into the Tn7 transposition vector pUC18T mini-Tn7T [18] to give pUC18T mini-Tn7T-omp1lux. The Tp-resistance gene from pFTP1 [18] was excised with *Kpn*I and cloned into the *Kpn*I site of pUC18T mini-Tn7T-omp1lux to give pUC18T mini-Tn7T-omp1lux-Tp^R. This latter plasmid was then transferred to *B. pseudomallei* by triparental filter-conjugation performed in the presence of SM10λ*pir*[pTNS2] with selection for Tp resistance and counterselection with streptomycin [18]. One such resulting *B. pseudomallei*::Tn7*omp-lux* derivative, designated "08-omp4," was used in the present study (figure 1*A*) and was assessed to be stable through ~100 generations in the absence of antibiotic. The intergenic site of insertion was determined to be located 25 nucleotides downstream of the stop codon of a *glmS2* [19].

Mice and experimental infection. Unanesthetized female BALB/c mice (age, 5–10 weeks) were intranasally infected by placement of 12 μL of bacteria onto the nostrils (6 μL per nostril). The inoculum contained 3.6×10^5 stationary phase cells resuspended in phosphate-buffered saline (PBS). Animals were monitored for signs of morbidity and were euthanized by use of terminal anesthetic or cervical dislocation. All protocols were

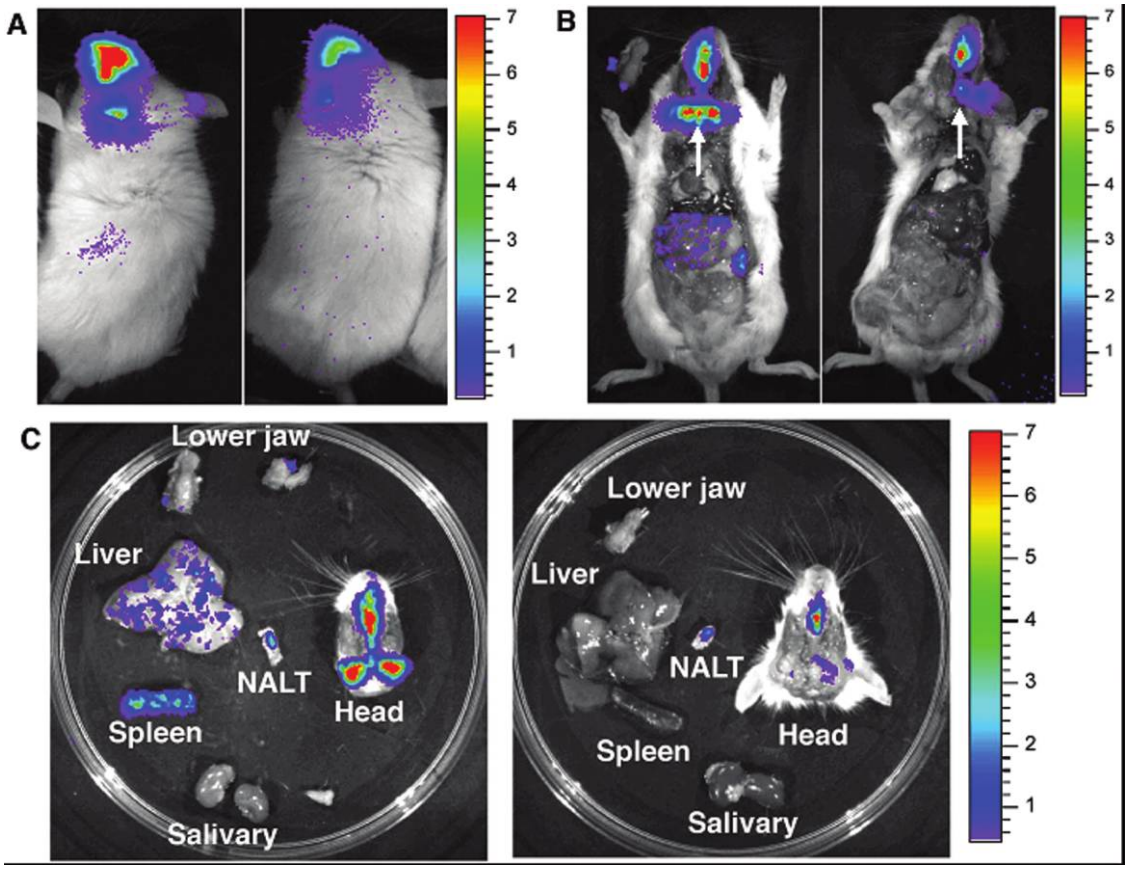

Figure 2. Bioluminescence imaging of mice at 48 h after infection. *A,* Live animal. *B,* The lower jaw removed and the soft tissue of the hard palate peeled back to expose the nasal cavity and nasal-associated lymphoid tissue (NALT) on the upper (posterior) surface of the hard palate. *C,* Dissected head and organs.

approved by the animal ethics committees of the Queensland Institute of Medical Research and Griffith University, in accordance with the guidelines of the National Health and Medical Research Council of Australia.

Extraction and quantitation of bacteria from mice. To determine the bacterial load, mice were euthanized at ~2, ~24, ~48, and ~72 h after inoculation. Organ and tissue specimens were surgically excised aseptically and homogenized in sterile PBS. Dilutions were plated on LB agar that contained streptomycin, and the bacterial loads (colony-forming units [cfu]) were determined. Some plates were examined to determine the bioluminescence of colonies; all observed colonies from a variety of organs (~3000) were luminescent, demonstrating complete stability of the mini-Tn7T::*lux* in vivo. In initial experiments, the whole brain was dissected from the cranium, including the olfactory bulb and the brain stem. In subsequent experiments, the olfactory bulb was dissected from the rest of the brain, which was dissected into 2 parts just rostral to the pons. The olfactory mucosa was dissected from the nasal cavity on both sides, by use of a dorsal and caudal approach. NALT was excised as described elsewhere [20, 21]. In brief, the palate was exposed and dissected from the underlying bone tissue and peeled back, exposing the NALT on the interior surface.

Bioluminescence imaging. Mice were anesthetized by subcutaneous injection of a ketamine-xylazine mixture and imaged by use of an IVIS charge-coupled device camera system (Xenogen) for 1–5 min. Bioluminescence was also observed in dissected mice with the NALT exposed (see previous section).

Tissue fixation and preparation for immunohistochemical analysis. While the mice were receiving terminal anaesthetic, at 2–72 h after inoculation, transcardial perfusion with 4% paraformaldehyde in 1× PBS was performed. Heads were then removed and postfixed overnight at room temperature. After fixation, the heads were decalcified in 20% disodium ethylenediaminetetraacetic acid in 1× PBS. The heads were prepared for Cryostat and polyethylene glycol (PEG) sectioning. For Cryostat sectioning, the heads were placed in an embedding matrix (O.C.T. compound; Miles Scientific) and snap-frozen by immersion in isopentane that had been cooled with liquid nitrogen. Cryostat sections (25 μm) of the nasal cavity and brain were cut, mounted onto gelatinized slides, and stored at −80°C. For PEG sectioning, after decalcification, the heads were embedded in

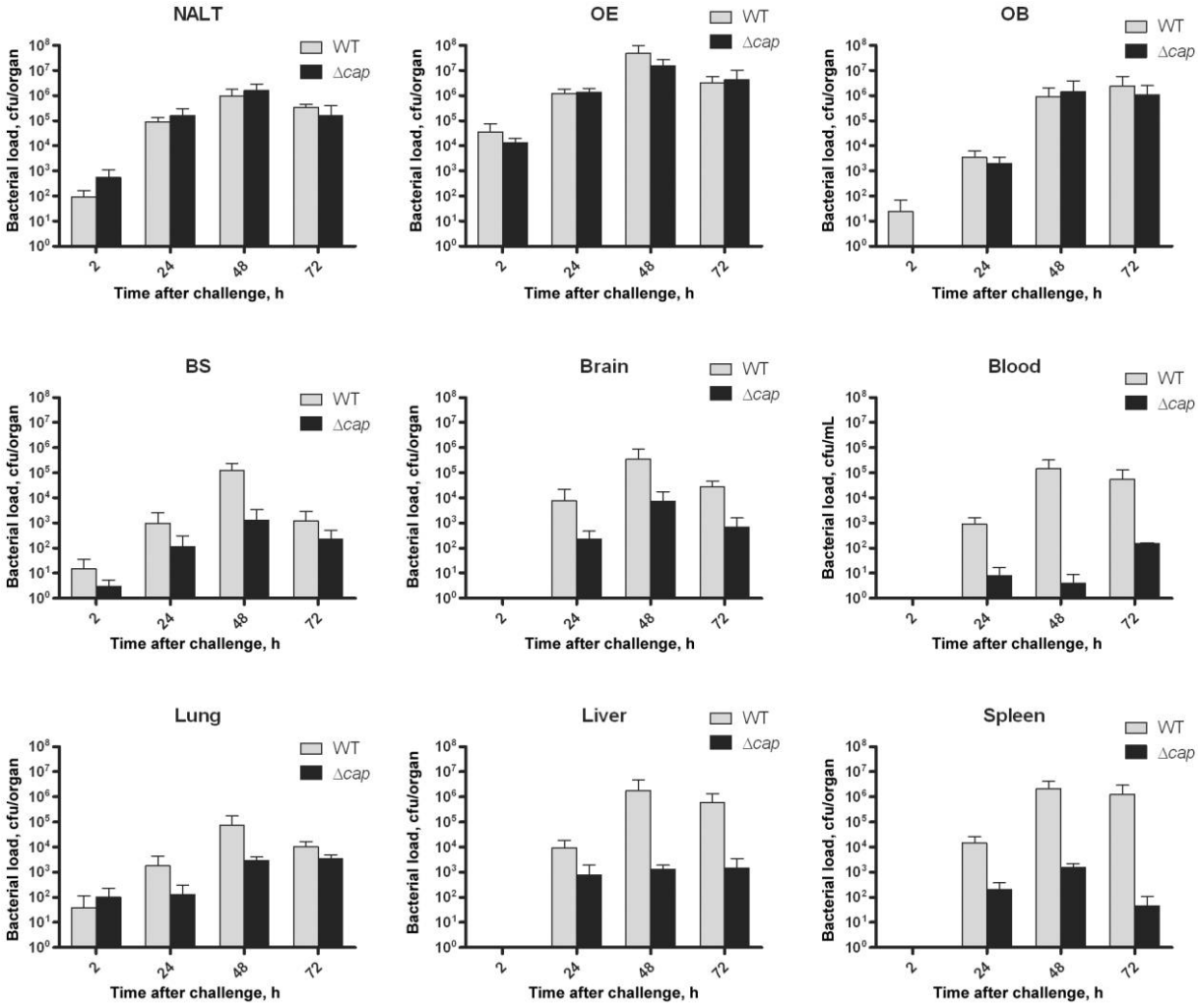

Figure 3. Determination of the bacterial load in the organs and tissues of mice at intervals after intranasal infection. Mice were infected with either strain 08 (wild-type [WT]) or a capsule-deficient mutant of 08 (Δ*cap*). "Brain" refers to the rest of the brain after dissection and removal of brain stem and olfactory bulbs. Data were derived from a group of 4 animals of each genotype and are expressed as the mean ± standard deviation. BS, brain stem; NALT, nasal-associated lymphoid tissue; OB, olfactory bulb; OE, olfactory epithelium.

PEG, as described elsewhere [22]; sectioned at 40 μm; and stored at 4°C before analysis.

Immunohistochemical analysis. Sections were incubated in dimethyl sulfoxide for 15 min before being washed with 0.1 mol/L PBS and 0.1% Triton X-100 for 5 min. They were then incubated with 10% normal donkey serum (Sigma) in 0.1 mol/L PBS with 0.1% Triton X-100 for 1 h at room temperature. The sections were incubated in primary antibodies (antiolfactory marker protein [1:1500; Wako], *B. pseudomallei* antisera [1:200] [23], and glial fibrillary acidic protein [1:300; Sigma]) diluted in 10% normal donkey serum/PBS/Triton X-100 overnight at room temperature. Sections were then washed with PBS/Triton X-100 and incubated in related secondary antibodies: donkey anti–goat Alexa Fluor 488 (1:400; Invitrogen), donkey anti–rabbit Alexa Fluor 594 (1:800; Invitrogen), and donkey anti–rabbit Alexa Fluor 488 (1:400; Invitrogen) antibodies, which were diluted in 0.1 mol/L PBS and 0.1% Triton-X-10 for 3 h at room temperature, washed in PBS/Triton X-100, and mounted with Vectashield 4',6-diamidino-2-phenylindole mounting medium.

Image capture and image preparation. Images were captured on an Axio Imager Z1 epifluorescence microscope with the use of Apotome and an Axiocam Mrm camera (Carl Zeiss). Serial optical sections were captured using AxioVision software, release 4.6 (Carl Zeiss MicroImaging), and were projected to provide 2-dimensional images of maximum brightness. Figures were compiled in Adobe Photoshop software (version 7.0) and Adobe Illustrator software (version 10.0).

RESULTS

Bioluminescence monitoring of* B. pseudomallei *infection in live animals reveals early nasopharyngeal replication. Thirty live mice that were infected with *B. pseudomallei*, as confirmed by organ

bacterial load and symptomology, consistently displayed bioluminescence in the nasopharyngeal region as early as 24 h after intranasal inoculation, with a substantial increase occurring 2–48 h after infection (figure 1*B*). This finding suggests that colonization of the mucosal epithelium occurs.

In situ visualization of bioluminescent* B. pseudomallei *in mice: infection of the nasal mucosa and NALT. To determine more precisely the sites of nasal mucosal replication, we euthanized and dissected animals at 2, 24, and 48 h after infection; subjected them to imaging; and determined the bacterial load in organs. We specifically examined the possibility that nasal-associated lymphoid tissue (NALT) might be a site of invasion and replication for *B. pseudomallei* and, hence, a portal of entry to distal sites, as is the case for some respiratory pathogens in mice and, with respect to the equivalent lymphoid tissue, in humans [12, 24]. We therefore excised the hard tissue of the soft palate, which is peeled back to expose NALT on the interior surface. Other organs were also dissected, and the live animal images that were obtained are shown for each corresponding dissection in figure 2A and 2*B*.

At 2 h after infection, no bioluminescence was detected. At 24 h after infection, bioluminescence was not seen in the region of the peeled-back palate where the NALT was exposed but, instead, was seen in the region from which the NALT had been resected (data not shown)—that is, within the nasal cavity.

At 48 h (figure 2*A* and 2*B*) and 72 h after infection, bioluminescence substantially increased, confirming further replication in the nasal mucosal epithelium. In addition, signal was seen in the region of the exposed NALT bounded by 1 or 2 foci of bioluminescence (figure 2*B*), which most likely denote the submandibular lymph nodes. At 48 h and 72 h after infection, bioluminescence was also apparent in the liver and spleen, where counts of $>5 \times 10^6$ cfu/organ were noted. This finding suggests that adherence and replication occurring in association with nasal mucosal epithelium and invasion of NALT are events occurring early after intranasal infection.

To further substantiate the latter hypothesis, we removed the tissue containing the NALT, as well as other organs (figure 2*C*). Bioluminescent imaging clearly showed a patch of bioluminescence in the isolated soft tissue of the hard palate, strongly suggesting infection of the NALT.

Determination of the bacterial load demonstrates replication in NALT. Determination of the bacterial load in the tissue specimens (data not shown) showed that substantial numbers of bacteria were found in NALT (mean load, 1.02×10^3 cfu/NALT specimen [$n = 14$]) (figure 3) as early as 2 h after infection. After 24 h, the bacterial count increased, reaching values of $>1 \times 10^6$ cfu/NALT specimen. What is striking about our results is that (1) even relatively soon after infection (i.e., 2 h after infection), bacteria were recovered from NALT; and (2) bacteria replicated at this site, as assessed by colony-forming unit counts determined at 24 h and 48 h after infection. We also observed replication in NALT with another strain of *B. pseudomallei* (strain 1026b), using intranasal inocula of 3×10^3 cfu and 3×10^4 cfu (data not shown). These results suggest a rapid tropism for the lymphoid tissue.

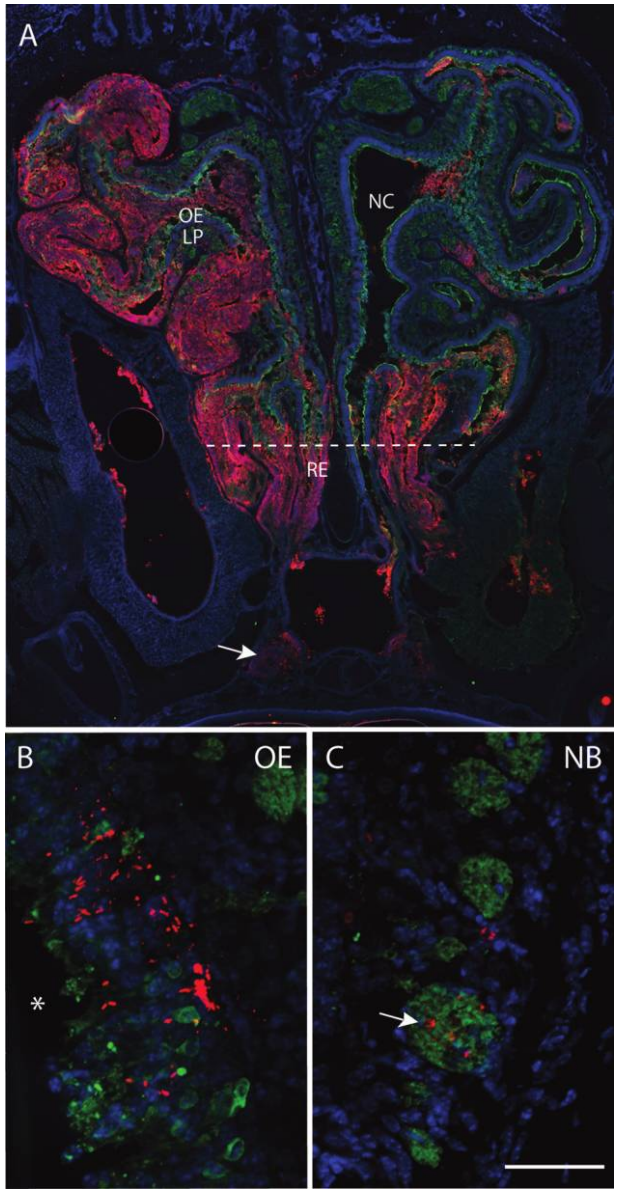

Figure 4. *Burkholderia pseudomallei* infection in the nasal cavity (NC). *A, B. pseudomallei (red)* seen throughout the NC at 48 h after inoculation. (Coronal section, dorsal is up). Olfactory sensory neurons are identified by expression of olfactory marker protein *(green)* in the olfactory epithelium (OE) and in the nerve bundles (NB) beneath it in the lamina propria (LP). *B. pseudomallei* infection is also present in the respiratory epithelium (RE; separated from the OE by a dashed line) and in the NALT *(arrow). B,* Higher-power magnification of the OE showing individual *B. pseudomallei* organisms *(red)* throughout the OE, from the surface (*) through to the LP, within which NB are immunolabeled for olfactory marker protein. *C, B. pseudomallei* identified within the LP, including within the NB *(arrowhead).* Nuclei are stained blue. Scale bar denotes 750 μm *(A)* and 50 μm (*B* and *C*).

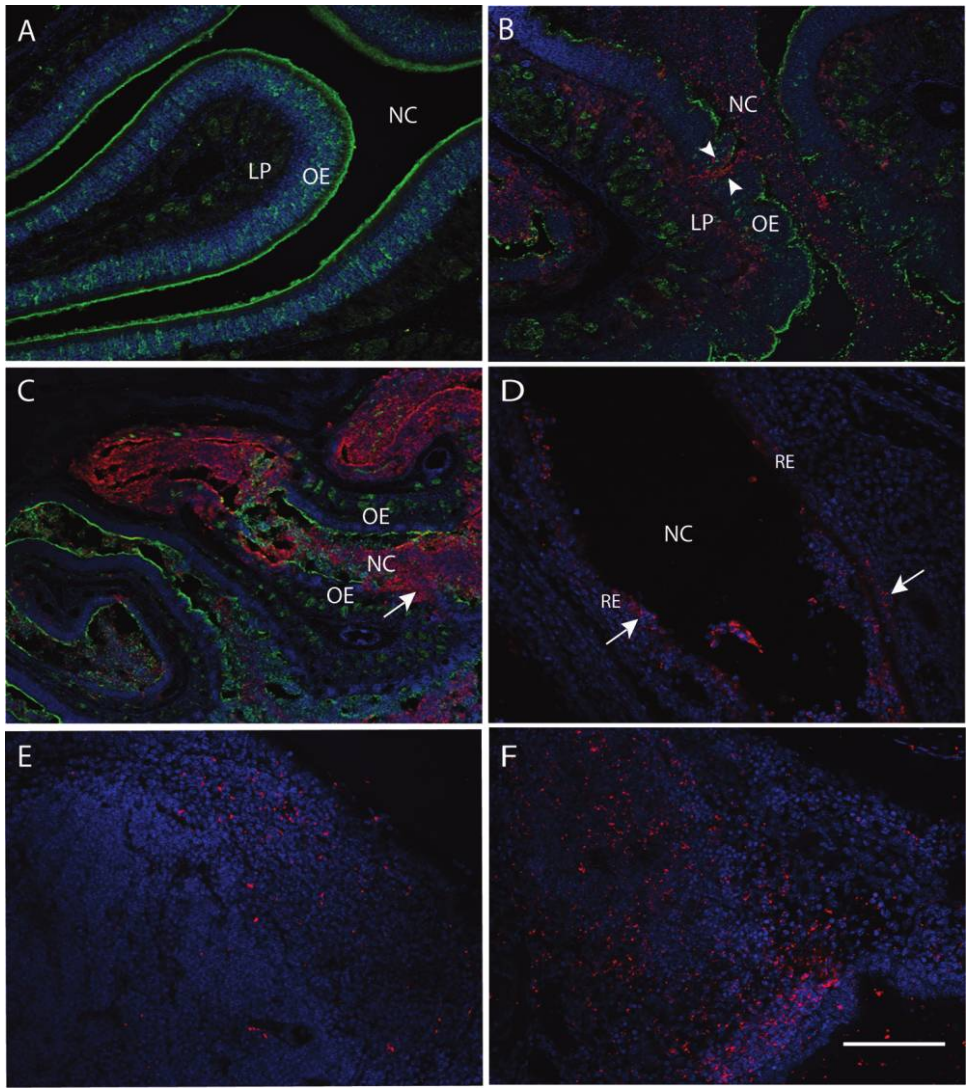

Figure 5. *Burkholderia pseudomallei* in the olfactory epithelium (OE), respiratory epithelium (RE), and nasal-associated lymphoid tissue (NALT). *A,* In an uninfected region, demonstration of the typical structure of the OE with a clear nasal cavity (NC) and expression of olfactory marker protein *(green). B,* At 24 h, an infected region of the NC is full of bacteria *(red)* and unidentified nuclei *(blue).* The OE is breached in places *(arrowheads),* leading to extensive colonization of the lamina propria (LP), without colonizing the epithelium above. *C,* At 48 h, some parts of the OE are lost completely and replaced by bacteria *(arrows). D,* Bacteria *(red)* in the RE at 24 h: a thinner morphology and absence of olfactory marker protein staining *(green)* confirm that this is RE *(arrows). E* and *F,* Coronal section through NALT at 24 h *(E)* and 48 h *(F)* after inoculation showing bacterial colonization *(red).* At 48 h, extensive replication of the bacteria is observed through NALT *(F).* Scale bar denotes 200 μm (*A* and *B*), 400 μm *(C),* and 100 μm (*D–F*).

B. pseudomallei *infection of the nasal cavity.* To determine the site(s) of colonization and also to confirm infection of the NALT, we examined infection in coronal sections obtained from infected mice at 48 h after infection. Two uninfected animals were used as control animals. Immunofluorescence microscopy was used to identify *B. pseudomallei* and a key marker protein of the olfactory epithelium and nerve bundles. Colonization of the nasal mucosal epithelium could potentially involve the respiratory and/or olfactory epithelium that occupy the approximately rostral one-third and more caudal two-thirds of the nasal mucosa, respectively. Figure 4*A* shows the nasal cavity at low magnification; there is extensive infection of the nasal cavity, which extends from the respiratory epithelium to the olfactory epithelium. Infection of NALT is also confirmed. Infection of the region lined by the olfactory epithelium is particularly extensive, and at higher-power magnification, *B. pseudomallei* infection is evident throughout the olfactory epithelium and within the nerve bundles in the lamina propria beneath the epithelium (figure 4*B* and 4*C*).

B. pseudomallei *in the olfactory epithelium, respiratory epithelium, and NALT.* Figure 5*A* shows the structure of the uninfected olfactory epithelium with the olfactory sensory neurons immunolabeled with olfactory marker protein. Bacteria were not observed in this region at 2 h after infection or in the

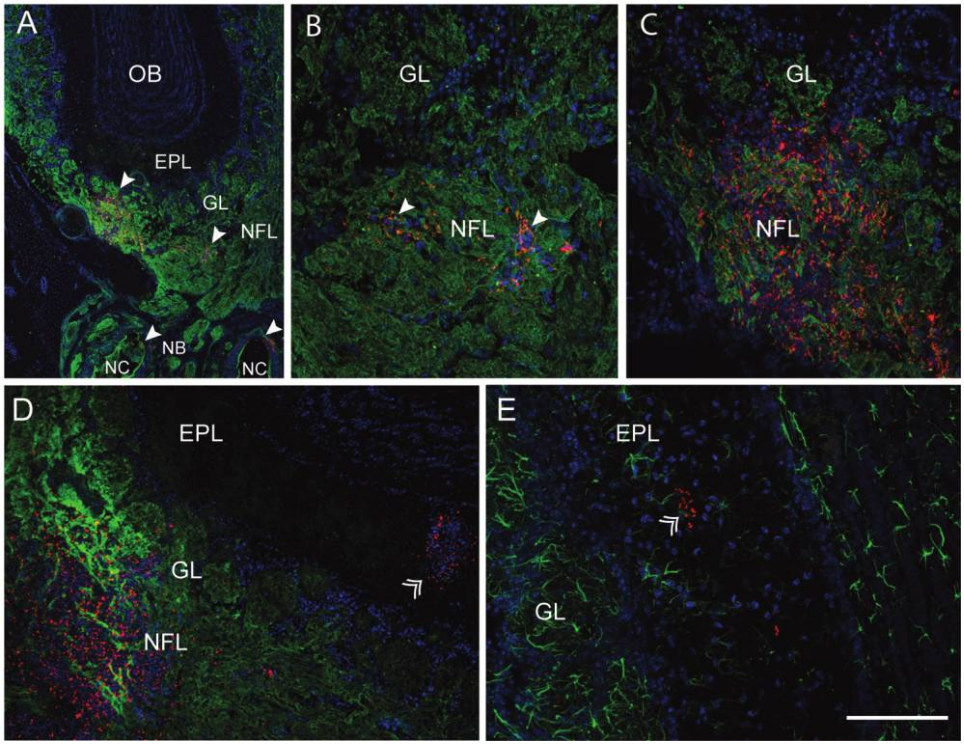

Figure 6. *Burkholderia pseudomallei* detected in the olfactory bulb (OB). *A,* At 48 h after inoculation, observation of *B. pseudomallei (red)* throughout the olfactory pathway *(green)* from the nasal cavity (NC) through to the OB in the brain *(arrowheads).* Bacteria are seen in the nasal cavity and olfactory epithelium and in the nerve fiber layer (NFL) and the glomerular layer (GL) of the OB. *B* and *C, B. pseudomallei* initially detected in the superficial parts of the OB, the NFL *(B, arrowheads),* and the GL. *D* and *E,* At 72 h after inoculation, detection of bacteria *(red)* not only in the NFL and the GL but also, on occasion, deeper in the OB within the external plexiform layer (EPL; *double arrowheads*). A high density of olfactory nerve terminals *(D, green)* and astrocytes *(E, green)* show the location of the GL. Nuclei are stained blue. Scale bar denotes 560 μm *(A),* 140 μm (*B* and *C*), 200 μm *(D),* and 100 μm *(E).* NB, nerve bundles.

sections obtained from control animals (data not shown). In the infected region, at 24 h after infection, the nasal cavity was replete with bacteria and unidentified nuclei (figure 5*B*), and the olfactory epithelium was disrupted, taking on a crenated appearance. The olfactory epithelium was breached in places, with bacteria extending through the multiple cell layers of the epithelium and colonizing the lamina propria (figure 5*B*), including the bundles of olfactory axons located ventral to the lamina propria (figure 4*C*). At 48 h after infection, some parts of the olfactory epithelium were completely disrupted and replaced by bacteria (figure 5*C*). Serial optical sections clearly demonstrated infection within the olfactory epithelium. The respiratory epithelium is also infected, seemingly to a lesser extent (figure 5*D*). Extensive colonization of the NALT was detected from 24 h after infection both in the sections through the olfactory cavity (figure 5*E* and 5*F*), as well as in whole mount specimens of the NALT (data not shown), which were excised as described above (figure 2).

B. pseudomallei *in olfactory sensory axons and the olfactory bulb.* Olfactory sensory neurons from the epithelium project to the olfactory bulb in the brain via the axons of the olfactory nerve, constituting a monosynaptic pathway to the brain. We therefore investigated whether bacteria were present in the olfactory nerve and the olfactory bulb. At 48 h after infection, bacteria were detected in the nerve fiber layer and the glomerular layer of the olfactory bulb (figure 6*A* and 6*C*), as well as in the nerve bundles within the olfactory mucosa (figure 4*C*). At 72 h after infection, bacteria were not only readily detected in the olfactory epithelium and olfactory axon bundles within the lamina propria of the olfactory mucosa and in the nerve fiber layer and glomeruli of the olfactory bulb but were also detected as clusters of cells in the deeper layers of the olfactory bulb (figure 6*D* and 6*E*).

Of significance, no bacteria were detected in blood at the earliest time point (2 h after infection), when measurable counts were observed in samples obtained from whole brain (data not shown). This suggested that, at this time, the brain was not infected by means of hematogenous spread.

In a second experiment conducted to assess the bacterial load in different organs and tissues, bacteria were detected in the olfactory mucosa (the epithelium plus the lamina propria) and the olfactory bulb (the rostral part of the brain)—but not in blood—at 2 h after infection (figure 3). The rest of the brain was bisected at the pons into a caudal section, which included the brain stem and cerebellum, and a rostral section, which included

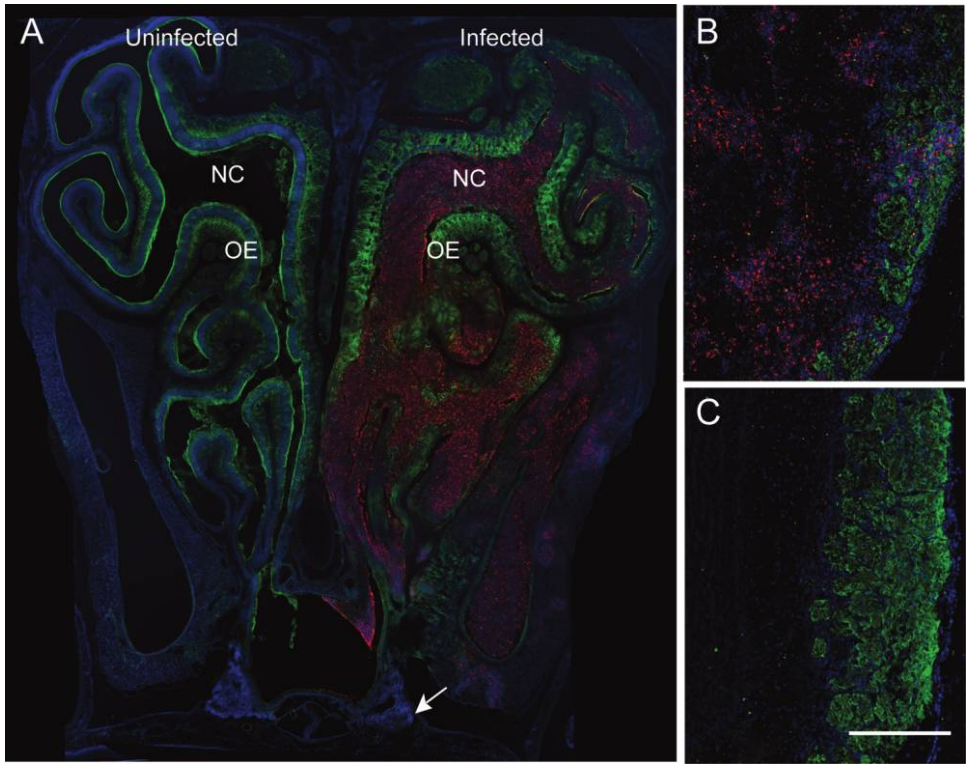

Figure 7. *Burkholderia pseudomallei* detected unilaterally in the olfactory system in one animal. *A,* At 72 h after intranasal inoculation, robust infection with bacteria *(red)* on one side of the nasal cavity (NC), including the olfactory epithelium (OE, identified by outer membrane protein immunoreactivity) *(green)* and nasal-associated lymphoid tissue *(arrow). B,* Bacteria *(red)* in the olfactory bulb on the same side as the infected NC. *C,* Olfactory bulb on the side of the uninfected NC devoid of bacteria. Nuclei are stained blue. Scale bar denotes 760 μm *(A)* and 200 μm (*B* and *C*).

the midbrain and cerebrum without the olfactory bulbs. The main, rostral section of the brain was free of bacteria, whereas low bacterial counts were observed in the brain stem section (figure 3).

Given these results, we hypothesized that the olfactory epithelium and nerve provide a direct pathway for *B. pseudomallei* to infect the brain, in the absence of hematogenous spread. To test this, we used a capsule-deficient mutant of *B. pseudomallei* 08, which survives in blood with very low efficiency and, consequently, causes very low levels of infection of the liver and spleen, compared with the wild-type strain [15]. We confirmed that this mutant colonized the blood very poorly but still robustly infected the nasal cavity (NALT and olfactory epithelium) and the brain (olfactory bulb and brain stem) (figure 3). An indirect test of this hypothesis was also provided by one animal in which colonization and replication occurred only in one side of the nasal cavity. Figure 7*A* shows, at 72 h after infection, extensive infection on the right side of the nasal cavity, in contrast to the contralateral side; consistent with this finding, images of higher-power magnification show that the NALT was much more extensively colonized on the infected side and that the olfactory epithelium was severely disrupted on the infected side only (data not shown). Most importantly, the olfactory bulb was infected only ipsilateral to the infection of the nasal cavity and NALT, suggesting a direct rather than systemic route of infection (figure 7*B* and 7*C*).

DISCUSSION

NALT is part of an integrated system of mucosa-associated lymphoid tissue, which also includes gut-associated lymphoid tissue, which is known to provide a portal of entry for some enteric pathogens [25]. Replication in NALT provides a direct route for dissemination to other organs via the bloodstream and lymphatic system. It is the only organized mucosal lymphoid tissue in the murine upper respiratory tract and is considered to be the equivalent of Waldeyer's ring in humans, functionally resembling human tonsils [20]. In this context, it is notable that pathogens of the upper respiratory tract, such as *Haemophilus influenzae* and *Streptococcus pneumoniae,* can infect tonsils in humans [26, 27] and that avian influenza A can infect ex vivo human upper respiratory tract tissues, including tonsillar tissue [24]. In addition, group A streptococcus also uses NALT as a portal of entry, and this may involve membranous cells [12]. We propose that NALT provides a portal of entry to the lymphatic system for *B. pseudomallei* in murine melioidosis and, by inference, the equivalent tissue in human. Whether membranous cells are involved remains a subject for future investigation.

Human melioidosis includes infections of the CNS [1, 5–7], and, in the present study, we found evidence of very rapid infection of the brain without initial detectable infection in blood. Immunohistological analysis revealed infection in the nerve bundles at 24 h after infection and in the olfactory bulb (i.e., the rostral brain) at 48 h. These data point to direct transmission from the olfactory epithelium to the olfactory bulb, without involvement of the blood. The capsule of *B. pseudomallei* is required for persistence in the blood when inoculated intraperitoneally in hamsters [15]. Our results show that capsule-deficient *B. pseudomallei* failed to significantly survive in blood after intranasal inoculation, confirming the importance of the capsule in systemic infection. In contrast, the capsule-deficient mutant colonized the olfactory epithelium and olfactory bulb, demonstrating a lack of capsule dependence for infection of neural tissues and confirming that systemic infection is not a prerequisite for CNS infection. This latter conclusion is strengthened by the observation of a case of unilateral infection of the olfactory epithelium and bulb in one animal in which the infection remained ipsilateral even at 72 h after infection. Infection of the brain via olfactory epithelium, although known for some viruses [28–30], rarely has been reported for bacteria [31]. We propose that this route of entry directly to the brain may be clinically important in some cases of CNS melioidosis.

There are 2 potential routes of entry into the CNS from the nasal cavity. Most favored by our data is the olfactory sensory nerve (cranial nerve I). A second route is via the trigeminal nerve, which widely innervates the nasal cavity throughout the respiratory and olfactory mucosae and innervates the brain stem. Our data favor the olfactory nerve as the primary route of entry into the CNS: compared with the extent of olfactory bulb infection, the extent of brain stem infection occurring after intranasal inoculation was minor. However, even a relatively minor amount of infection of the trigeminal nerve by *B. pseudomallei* would deliver bacteria directly to the brain stem, a site of human neurological melioidosis. Brain stem infection could also be a secondary consequence of CNS infection via the olfactory nerve. It has been suggested that *Listeria monocytogenes* can cause brain stem encephalitis in sheep by neuronal transport via the trigeminal nerve [32]. Access to the brain via the olfactory nerve was also indicated after mice were intranasally infected with *S. pneumoniae* because bacterial load in neuronal tissues (and the NALT) was identified in the absence of bacteremia [31].

The mechanism of travel of *B. pseudomallei* along nerves is not known. Possible mechanisms are travel within the sensory axons or travel within the glial cells surrounding the sensory neurons, the olfactory-ensheathing cells surrounding the olfactory nerve, and the Schwann cells surrounding the trigeminal nerve. There is good evidence that olfactory ensheathing cells are actively involved in immunologic protection against pathogens from the nasal cavity [33, 34]. Actin-based motility of *B. pseudomallei* [35] may be involved in intracellular movement in sensory axons or in glia. Another possible mechanism of transportation along the nerves is motility within the perineurium surrounding the nerve bundle. In rodents, the perineurium of the olfactory nerve is connected with the epidural space surrounding the brain [36, 37], which could allow direct access of bacteria to the brain if the bacteria penetrate the olfactory mucosa.

The initial interaction of *B. pseudomallei* with the mucosal epithelium and the severe disruption of the olfactory epithelium after infection strongly merit further investigation. Although strong adherence of *B. pseudomallei* to cultured cell lines has not been demonstrated, in the absence of microcolony formation [16] (C.-A. Logue and I. R. Beacham, unpublished data), it is possible that a specific receptor-mediated association is a prerequisite for invasion. Invasion may also occur via structures specific to the olfactory epithelium, such as Bowman's gland ducts, perhaps explaining "patchy" invasion (figure 5*B*). Disruption of the olfactory epithelium may be the result of an inflammatory response, perhaps involving interaction with Toll-like receptor 2 [38].

Our results may have implications for vaccine development, because mucosal vaccination might be particularly effective [21, 39]. It has been reported that certain lectins reduce colonization of NALT by group A streptococcus [12]; if such carbohydrate interactions are also important in colonization by *B. pseudomallei,* they might be a target for novel prophylactic strategies.

Acknowledgment

This article is respectfully dedicated to the memory of our coauthor Robert Hirst.

References

1. White NJ. Melioidosis. Lancet **2003**; 361:1715–20.
2. Wiersinga WJ, van der Poll T, White NJ, Day NP, Peacock SJ. Melioidosis: insights into the pathogenicity of *Burkholderia pseudomallei.* Nat Rev Microbiol **2006**; 4:272–82.
3. Stone R. Infectious disease: racing to defuse a bacterial time bomb. Science **2007**; 317:1022–4.
4. Currie BJ, Jacups SP. Intensity of rainfall and severity of melioidosis, Australia. Emerg Infect Dis **2003**; 9:1538–42.
5. Currie BJ, Fischer DA, Howard DM, Burrow JNC. Neurological melioidosis. Acta Trop **2000**; 74:145–51.
6. Koszyca B, Currie BJ, Blumbergs PC. The neuropathology of melioidosis: two cases and a review of the literature. Clin Neuropathol **2004**; 5: 195–203.
7. Chadwick DR, Ang B, Sitoh YY, Lee CC. Cerebral melioidosis in Singapore: a review of five cases. Trans R Soc Trop Med Hyg **2002**; 96:72–6.
8. Leakey A, Ulett GC, Hirst RG. BALB/c and C57BL/6 mice infected with virulent *Burkholderia pseudomallei* provide contrasting animal models for the acute and chronic forms of human melioidosis. Microb Pathog **1998**; 24:69–75.
9. Hoppe I, Brenneke B, Rohde, M, et al. Characterization of a murine model of melioidosis: comparison of different strains of mice. Infect Immun **1999**; 67:2891–900.
10. Contag CH, Contag PR, Mullins JI, Spilman SD, Stevenson DK, Benaron DA. Photonic detection of bacterial pathogens in living hosts. Mol Microbiol **1995**; 18:593–603.

11. Doyle TC, Burns SM, Contag CH. *In vivo* bioluminescence imaging for integrated studies of infection. Cell Microbiol **2004**; 6:303–17.
12. Park H-S, Francis KP, Yu J, Cleary PP. Membranous cells in nasal-associated lymphoid tissue: a portal of entry for the respiratory mucosal pathogen group A streptococcus. J Immunol **2003**; 171:2532–7.
13. Brown NF, Beacham IR. Cloning and analysis of genomic differences unique to *Burkholderia pseudomallei* by comparison with *Burkholderia thailandensis.* J Med Microbiol **2000**; 49:993–1001.
14. Holden MTG, Titball RW, Peacock SJ, et al. Genomic plasticity of the causative agent of melioidosis, *Burkholderia pseudomallei.* Proc Natl Acad Sci U S A **2004**; 101:14240–5.
15. Reckseidler-Zenteno SL, DeVinney R, Woods DE. The capsular polysaccharide of *Burkholderia pseudomallei* contributes to survival in serum by reducing complement factor C3b deposition. Infect Immun **2005**; 73: 1106–15.
16. Boddey JA, Flegg CP, Day CJ, Beacham IR, Peak IR. Temperature-regulated microcolony formation by *Burkholderia pseudomallei* requires *pilA* and enhances association with cultured human cells. Infect Immun **2006**; 74:5374–81.
17. Meighen EA, Szittner RB. Multiple repetitive elements and organization of the *lux* operons of luminescent terrestrial bacteria. J Bacteriol **1992**; 174:5371–81.
18. Choi K-H, Gaynor JB, White KG, et al. A Tn7-based broad-range bacterial cloning and expression system. Nat Methods **2005**; 2:443–8.
19. Choi K-H, Mima T, Casart-Quintero Y, Rholl D, Beacham IR, Schweizer HP. Genetic tools for select-agent-compliant manipulation of *Burkholderia pseudomallei.* Appl Env Microbiol **2008**; 74:1064–75.
20. Asunuma H, Thompson AH, Iwasaki T, et al. Isolation and characterization of mouse nasal-associated lymphoid tissue. J Immunol Methods **1997**; 202:123–31.
21. Wu H-Y, Nguyen HH, Russell MW. Nasal lymphoid tissue (NALT) as a mucosal immune inductive site. Scand J Immunol **1997**; 46:506–13.
22. Robinson AJ, Meedeniya AC, Hemsley KM, Auclair D, Crawley AC, Hopwood JJ. Survival and engraftment of mouse embryonic stem cell-derived implants in the guinea pig brain. Neurosci Res **2005**; 53:161–8.
23. Boddey JA, Day CJ, Flegg CP, et al. The bacterial gene *lfpA* influences the potent induction of calcitonin receptor and osteoclast-related genes in *Burkholderia pseudomallei*-induced TRAP-positive multinucleated giant cells. Cell Microbiol **2007**; 9:514–31.
24. Nicholls JM, Chan MCW, Chan WY, et al. Tropism of avian influenza A (H5N1) in the upper and lower respiratory tract. Nat Med **2006**; 13: 147–9.
25. Sansonetti PJ, Phalipon A. M cells as ports of entry for enteroinvasive pathogens: mechanisms of interaction, consequences for the disease process. Semin Immunol **1999**; 11:193–203.
26. Lindroos R. Bacteriology of the tonsil core in recurrent tonsillitis and tonsillar hyperplasia—a short review. Acta Otolaryngol Suppl **2000**; 120:206–8.
27. Osterlund A, Popa R, Nikkilā T, Scheynius A, Engstrand L. Intracellular reservoir of *Streptococcus pyogenes* in vivo: a possible explanation for recurrent pharyngotonsillitis. Laryngoscope **1997**; 107:640–8.
28. Barnett E, Perlman S. The olfactory nerve and not the trigeminal nerve is the major site of CNS entry for mouse hepatitis virus, strain JHM. Virology **1993**; 194:185–91.
29. Plakhov IV, Arlund EE, Aoki C, Reiss CS. The earliest events in vesicular stomatitis virus infection of the murine olfactory neuroepithelium and entry of the central nervous system. Virology **1995**; 209:257–62.
30. Mori I, Goshima F, Ito H, et. al. The vomeronasal chemosensory system as a route of neuroinvasion by herpes simplex virus. Virology **2005**; 334: 51–8.
31. Van Ginkel FW, McGhee JR, Watt JM, Campos-Torres A, Parish L, Briles DE. Pneumococcal carriage results in ganglioside-mediated olfactory tissue infection. Proc Natl Acad Sci U S A **2003**; 100:14363–7.
32. Dons L, Jin Y, Kristensson K, Rottenberg ME. Axonal transport of *Listeria monocytogenes* and nerve-cell-induced bacterial killing. J Neurosci Res **2007**; 85:2529–37.
33. Vincent AJ, Choi-Lundberg DL, Harris JA, West AK, Chuah MI. Bacteria and PAMPs activate nuclear factor κB and Gro production in a subset of olfactory ensheathing cells and astrocytes but not in Schwann cells. Glia **2007**; 55:905–16.
34. Leung JYK, Chapman JA, Harris JA, et al. Olfactory ensheathing cells are attracted to, and can endocytose, bacteria. Cell Mol Life Sci **2008**; 65: 2732–9.
35. Stevens MP, Stevens JM. Jeng RL, et al. Identification of a bacterial factor required for actin-based motility of *Burkholderia pseudomallei.* Mol Microbiol **2005**; 56:40–53.
36. Nagra G, Koh L, Zakharov A, Armstrong D, Johnston M. Quantification of cerebrospinal fluid transport across the cribriform plate into lymphatics in rats. Am J Physiol Regul Integr Comp Physiol **2006**; 291: R1383–9.
37. Walter BA, Valera VA, Takahashi S, Ushiki T. The olfactory route for cerebrospinal fluid drainage into the peripheral lymphatic system. Neuropathol Appl Neurobiol **2006**; 32:388–96.
38. Wiersinga WJ, Wieland CW, Dessing MC, et al. Toll-like receptor 2 impairs host defense in gram-negative sepsis caused by *Burkholderia pseudomallei* (melioidosis). PLoS Med **2007**; 4:e248.
39. Hou Y, Hu W-G, Hirano T, Gu X-X. A new intra-NALT route elicits mucosal and systemic immunity against *Moraxella catarrhalis* in a mouse challenge model. Vaccine **2002**; 20:2375–81.